

Consideration of spectroscopic measurements with broadband Fourier domain mode-locked laser with two semiconductor optical amplifiers at ~1550 nm

Tatsuya Yamaguchi^{a,*}, Akira Nakamoto,^b and Yukitaka Shinoda^a

^aNihon University, College of Science and Technology, Department of Electrical Engineering, Tokyo, Japan

^bNihon University, Graduate School of Science and Technology, Department of Electrical Engineering, Tokyo, Japan

Abstract. In this study, an experimental system was developed using a broadband wavelength-swept laser for fast and broadband spectroscopic measurements at ~1550 nm. The broadband wavelength-swept laser employed Fourier domain mode-locking (FDML) to realize a high-speed sweep rate of 50.7 kHz. FDML lasers at ~1550 nm experience a problem of the sweep bandwidth being limited by the amplification wavelength range of the semiconductor optical amplifier (SOA). To realize a sweep bandwidth >100 nm, the proposed broadband FDML laser incorporated SOAs with different amplification wavelength ranges in parallel. Consequently, it expanded the sweep bandwidth to 120 nm at a center wavelength of 1544 nm. The experimental system employed the broadband FDML laser and introduced reference and compensation optics. These optics can compensate for the effects of fluctuations in optical output intensity and wavelength shift in the laser to improve measurement stability. Moreover, the experimental system demonstrated fast transmission spectrum measurements with a wavelength range of 1500 to 1580 nm. © The Authors. Published by SPIE under a Creative Commons Attribution 4.0 International License. Distribution or reproduction of this work in whole or in part requires full attribution of the original publication, including its DOI. [DOI: [10.1117/1.OE.62.3.036101](https://doi.org/10.1117/1.OE.62.3.036101)]

Keywords: fiber lasers; tunable lasers; near-infrared spectroscopy; optical systems; fiber optic sensors.

Paper 20221113G received Sep. 26, 2022; accepted for publication Feb. 14, 2023; published online Mar. 6, 2023.

1 Introduction

Near-infrared spectroscopy has a wide range of applications in structural chemistry, process analysis, agriculture, food, and medicine.¹⁻⁴ These applications using near-infrared light are advantageous in using materials such as highly durable and inexpensive glass and optical fiber. Further, using optical fibers as probes, flexible systems can be developed for nondestructive *in-situ* analysis. In recent years, the field of combustion systems has witnessed increasing interest in the elucidation of combustion mechanisms and the development of diagnostic techniques through the analysis of gas composition, temperature, pressure, and velocity.^{5,6} Therefore, gas analysis using a wide variety of lasers, such as vertical cavity surface emitting, supercontinuum, and frequency comb lasers, has been reported.⁷⁻⁹ However, for an in-depth understanding of the combustion mechanism, measurements in very transient combustion and propulsion environments at high pressure are required.^{6,10} Consequently, a measurement method with improved time resolution and an expanded measurement wavelength range must be established.

A gas temperature measurement method using a Fourier domain mode-locked (FDML) laser with a wavelength of 1300 nm has been reported as a high time-resolution measurement method.¹¹ The FDML laser comprises a fiber ring cavity, and the time of light circulating in the ring is controlled via a delay fiber. This optical control produces a high measurement rate of over several tens of kHz.¹² The ring cavity inserts a wavelength filter and a semiconductor optical amplifier, which together provide fast wavelength tuning and amplification, thereby

*Address all correspondence to Tatsuya Yamaguchi, yamaguchi.tatsuya@nihon-u.ac.jp

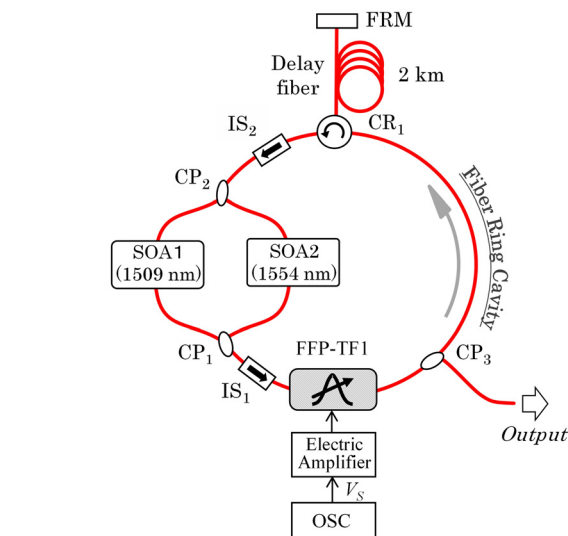
resulting in an excellent wavelength sweep capability. A previous study reported real-time spectral measurement systems with an FDML laser with a sweep bandwidth of 30 nm at 1550 nm.¹³ However, the sweep wavelength range in FDML lasers is limited by the amplification wavelength range of the semiconductor optical amplifier (SOA). Recently, in the medical field of optical coherence tomography, a broadband FDML laser of ~1300 nm was developed by arranging SOAs with different amplification wavelength ranges in parallel to overcome the limitation of the amplification wavelength range.^{14,15} Near-infrared spectroscopy has significantly contributed to the development of application fields by covering a wide range of wavelengths and improving measurement performance through the development of various lasers. Therefore, the application of the fast and broadband FDML laser to near-infrared spectroscopy for expanding the laser to the wavelength range of 1550 nm is a significant research prospect. In the 1520- to 1620-nm wavelength regions, numerous rotational vibration spectra exist. Mance et al.¹⁶ reported the transient absorption spectrum measurements of acetylene–oxygen gas mixtures during combustion.

This study aimed to develop a broadband FDML laser with a wavelength of ~1550 nm, wherein two SOAs were arranged in parallel to achieve high temporal resolution and to expand the measurement wavelength range for near-infrared spectroscopy. The developed broadband FDML laser uses two SOAs with center wavelengths of 1509 and 1554 nm to achieve a broadband sweep bandwidth of 120 nm at a center wavelength of 1544 nm and a high-speed sweep rate of 50.7 kHz. The experimental system using the broadband FDML laser introduced reference and compensation optics, which compensated for laser fluctuations and contributed to the stabilization of spectroscopic measurements. Moreover, the experiments demonstrated fast and broadband spectroscopic measurements of fast transmission spectra using fiber Bragg gratings (FBGs)^{17–20} that reflected only a specific wavelength region to simulate the absorption spectrum of a gas.

2 Broadband FDML Laser with Two SOAs

2.1 Optical Setup of Broadband FDML Laser

Figure 1 shows a broadband FDML laser. The laser comprises a fiber ring cavity with a circulator (CR), isolator (IS), coupler (CP), fiber Fabry–Perot tunable filter (FFP-TF1), and two SOAs.



Abbreviation

SOA: Semiconductor optical amplifier; CP: coupler; IS: isolator; FFP-TF: fiber Fabry-Perot tunable filter; CR: circulator; FRM: Faraday rotator mirror; OSC: oscillator; V_s : sweep control signal

Fig. 1 Broadband FDML laser with two SOAs.

SOA1 (SOA1013, Thorlabs) has a center wavelength of 1509 nm and a small signal gain of 13 dB; SOA2 (SOA1117, Thorlabs) has a center wavelength of 1554 nm and a small signal gain of 20 dB. Broadband spontaneous emission light is emitted from each SOA and entered the FFP-TF1 via CP₁ and IS₁. FFP-TF1 (Micron) has a full width half maximum (FWHM), center wavelength, and free spectral range of 85 pm, 1575 nm, and 190 nm, respectively. The FFP-TF1 extracted only light in a specific wavelength range. The light was repeatedly injected into SOAs while circling, and was gradually amplified to result in laser oscillation. The oscillator (OSC, 33612A, Agilent) controlled the wavelength range extracted by the FFP-TF1 using a sweep control signal (V_S).

In the experiment, the FFP-TF1 was controlled by V_S set to a sinusoidal signal with sweep speed $f_m = 50.7$ kHz and sweep period $T_m = 19.7$ μ s ($= 1/f_m$). The laser swept from short to long wavelength (forward scan) and from long to short wavelength (backward scan). In the ring cavity, a 2-km long delay fiber with a Faraday rotated mirror was installed to enable the laser to control the time for the light to circulate to ~ 19.7 μ s ($= T_m$) and synchronize it with the sweep period of the FFP-TF1. Thus, a high-speed sweep with the FDML operation was realized.^{12,20} The FFP-TF1 and the delay fiber were placed in a thermostatic chamber and maintained at a constant temperature of 25°C.²⁰ However, achieving a broadband sweep beyond 100 nm is challenging with the amplification wavelength range of a single SOA at 1550 nm. Thus, to overcome this limitation, the broadband FDML laser was developed by arranging two SOAs in parallel with different amplification wavelength ranges.

2.2 Characteristics of Broadband FDML Laser

First, to evaluate the optical output characteristics of the developed broadband FDML laser, the optical output was measured using an optical spectrum analyzer (OSA, AQ6317B, ANDO) with an averaging count of 10 for the single and parallel SOA cases (Fig. 2). When only SOA1 (center wavelength of 1509 nm) was connected excluding CP₁ and CP₂, a sweep bandwidth of ~ 70 nm was obtained on the short wavelength side; however, optical output at longer wavelengths above 1580 nm was not obtained. In the case of only SOA2 (center wavelength of 1554 nm), in contrast to SOA1, optical output was obtained at the long wavelength side and not at the short wavelength side. Thus, a laser using a single SOA at ~ 1550 nm cannot achieve a broadband sweep bandwidth beyond 100 nm owing to the limitation of the amplification wavelength range. However, using SOA1 and SOA2 in parallel can aid in the realization of a broadband sweep covering a wide range from short to long wavelengths. The developed broadband FDML laser achieved a broad sweep bandwidth of ~ 120 nm from 1484.3 to 1603.7 nm at a center wavelength of 1544 nm. In this configuration, each SOA amplified short and long wavelengths. For example, when a short wavelength light entered CP₂, 50% of the light was amplified by SOA1; however, the remaining 50% may not be amplified properly by SOA2. This results in the optical output intensity in broadband FDML lasers being lower than in lasers with a single SOA.

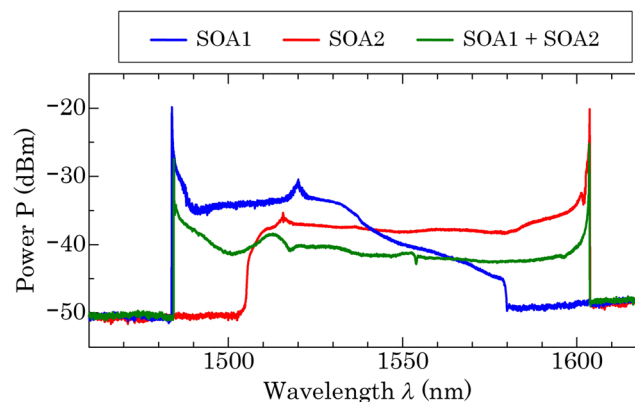


Fig. 2 Output spectrum of broadband FDML laser.

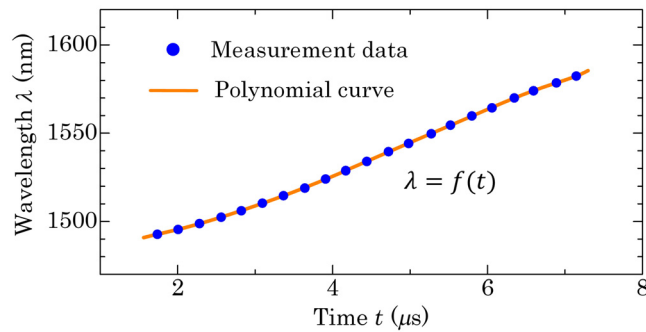


Fig. 3 Sweep characteristics of broadband FDML laser with forward-scan.

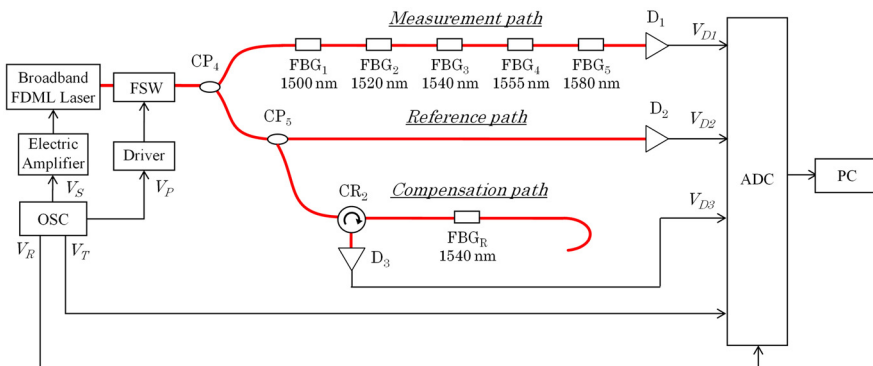
The wavelength sweep characteristics of the broadband FDML laser was further evaluated in an experimental setup using a wavelength filter with an FFP-TF2 and OSA.^{20–22} The FFP-TF2 (Micron) had a FWHM, center wavelength, and free spectral range of 119 pm, 1550 nm, and 120 nm, respectively. Figure 3 shows the measured results of the forward scan region of the broadband FDML laser. The broadband FDML laser operated at a high speed at a sweep rate of 50.7 kHz and achieved a sinusoidal broadband wavelength sweep. The sweep characteristics $f(t)$ of the broadband FDML laser can be approximated by a polynomial, yielding a time-to-wavelength conversion equation, which was used for spectroscopic measurements.

3 Experimental System with Broadband FDML Laser for Spectroscopic Measurements

3.1 Experimental Setup

Figure 4 shows an experimental system using the broadband FDML laser. The sinusoidal wavelength-swept light of the broadband FDML laser propagated through the optical fiber and entered a fiber optic switch (FSW). The FSW (NSSW, Agiltron) controls optical output ON/OFF with a repetition rate of DC ~ 500 kHz. The FSW extracted only the light in the forward scan region of the broadband FDML laser using the pulse control signal (V_P) of the OSC. Subsequently, the extracted light was injected into CP₄.

The optical system in the experimental system comprised three optical paths: measurement, reference, and compensation optical paths. In the measurement optical path, five FBGs with different reflection wavelengths were installed to simulate the absorption spectrum. The Bragg wavelengths of the FBGs were selected as 1500, 1520, 1540, 1555, and 1580 nm, with FWHM and reflectance of ~0.2 nm and 80%, respectively. With this configuration, the performance of



Abbreviation

FSW: Fiber switch; CP: coupler; CR: circulator; FBG: fiber Bragg grating; D: detector; OSC: oscillator; ADC: analogue-digital converter; PC: personal computer; V_D : detector signal; V_S : sweep control signal; V_P : pulse control signal; V_T : trigger signal; V_R : reference clock signal.

Fig. 4 Experimental system with broadband FDML laser.

the experimental system can be evaluated by simulating, for example, the absorption spectrum distributed around 1550 nm found in a mixture of acetylene and oxygen. This approach is easier to evaluate the quantitative performance of an experimental system that controls gas temperature and pressure, because the transmission spectrum of FBG can be easily controlled by the application of strain. For stable continuous measurement of the experimental system, the effects of fluctuations in optical output intensity and wavelength shift of the broadband FDML laser must be considered. The reference optical path directly monitored the laser output to correct fluctuations in optical output. Further, the compensation optical path was set up with an FBG_R (Bragg wavelength of 1540 nm and FWHM and reflectance of ~0.2 nm and 80%, respectively) as the reference wavelength. The experimental system compensated for the effect of wavelength shift of the broadband FDML laser by monitoring changes in the reflection spectrum of the FBG_R.

The light from each optical path entered the detector (*D*) and the detector signal (*V_D*) was input to an analog-to-digital converter (ADC). The ADC (5170R, National Instruments) has four analog input channels with sampling frequency and resolution of 250 MHz and 14 bits, respectively. The ADC was input with the trigger signal *V_T* and the reference clock signal *V_R* synchronized with the sweep control signal *V_S* of the broadband FDML laser. In addition, the acquisition timing of the *V_D* was controlled. Moreover, the broadband FDML laser was operated with a sweep rate of 50.7 kHz and a sweep bandwidth of 120 nm in forward scan, and spectroscopic measurements were performed using FBGs.

3.2 Compensation Method of Wavelength Shift of Broadband FDML Laser

Experimental systems using broadband FDML lasers experience spectral measurement accuracy degradation because of wavelength shift of the laser caused by long-time operation. This must be resolved to promote the development of monitoring applications that require continuous measurement. Consequently, a correction method using FBG_R was considered. Figure 5(a) shows the wavelength sweep characteristics of the broadband FDML laser, Fig. 5(b) shows the reflection signal of the FBG_R, and Fig. 5(c) shows the signal processing flow for the compensation. Assuming the wavelength sweep characteristic *f(t)* of the broadband FDML laser with no wavelength shift, reflection signal was detected at time *t_R* from the FBG_R with Bragg wavelength *λ_R*. Whereas, in the case of a broadband FDML laser whose wavelength has shifted by *Δλ_S* owing to long-time operation, the wavelength sweep characteristic changed to *f'(t)* and the reflection signal time changed from *t_R* to *t_m*. In the correction process flow, the wavelength shift *Δλ_S* of the laser can be calculated using the following Eq. (1) by measuring the time *t_m* of the reflection signal

$$\Delta\lambda_S = f(t_R) - f(t_m). \tag{1}$$

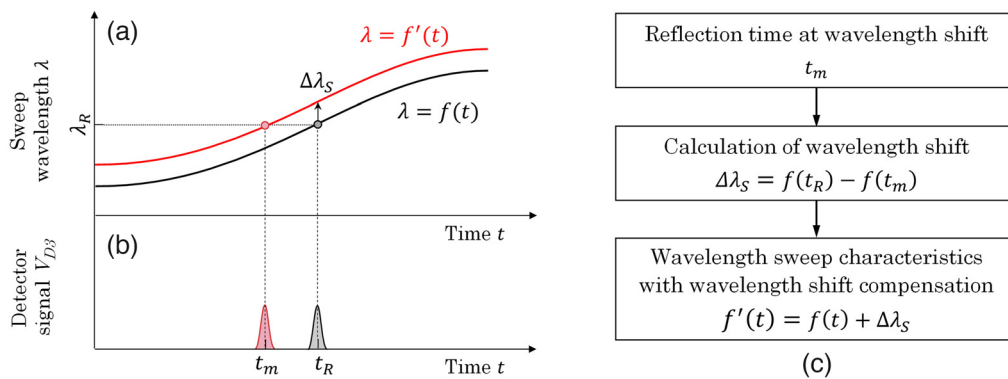


Fig. 5 Method of compensating for wavelength shift of broadband FDML laser. (a) Wavelength sweep characteristics of broadband FDML laser; (b) reflection signals of FBG_R; and (c) signal processing flow for compensation.

Further, using the wavelength shift $\Delta\lambda_S$, the wavelength sweep characteristic $f'(t)$ can be calculated using the following Eq. (2) when the laser wavelength shift occurs

$$f'(t) = f(t) + \Delta\lambda_S. \quad (2)$$

As this method measures only one point of the FBG_R reflection signal, the compensation process can be performed at a low computational cost. The experiment corrected the wavelength sweep characteristic $f(t)$ obtained in Fig. 3 via processing using FBG_R to calculate the wavelength sweep characteristic $f'(t)$, which compensated for the effect of wavelength shift.

4 Experimental Results

4.1 Spectroscopic Measurements with Broadband FDML Laser

First, the light output of each optical path was evaluated using the experimental system. Figure 6 shows the results of the detector signal when the broadband FDML laser was swept for one cycle with the sweep period $T_m = 19.7 \mu\text{s}$. Only light in the forward scan region of the broadband FDML laser was extracted by the FSW. Figure 6(a) shows the measurement signal by V_{D1} , and transmission signals by five FBGs with different Bragg wavelengths were observed. However, the measurement signal was affected by fluctuations in the optical output of the broadband FDML laser. Therefore, as shown in Fig. 6(b), the experimental system directly measured the optical output of the broadband FDML laser as a reference signal with V_{D2} . In Fig. 6(c), the reflection signal of the FBG_R was detected as a compensation signal with V_{D3} to compensate for the effect of the laser wavelength shift. When the broadband FDML laser was wavelength-shifted, the effect was eliminated by adapting the signal processing shown in Fig. 5 on the FBG_R reflection signal.

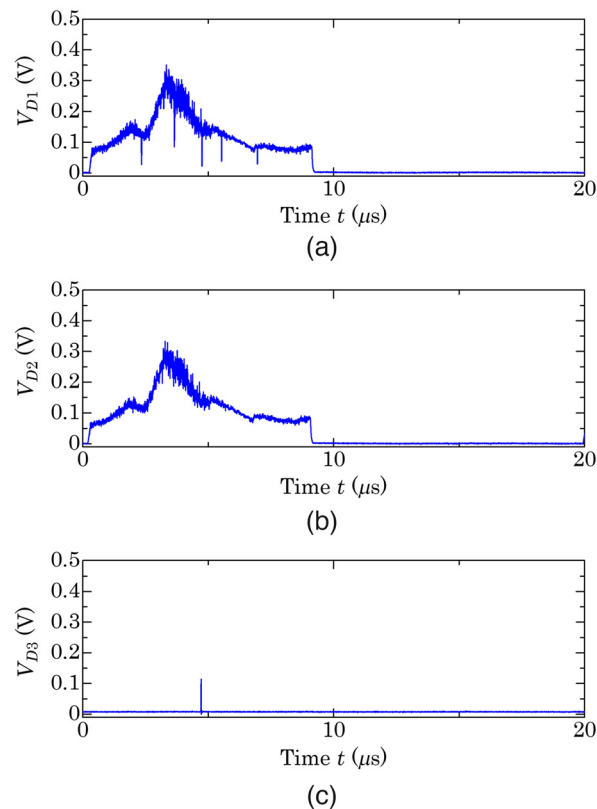


Fig. 6 Detector signals of experimental system. (a) Measurement path; (b) reference path; and (c) compensation path.

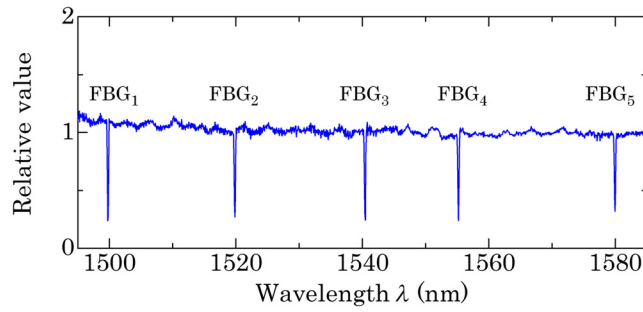


Fig. 7 Spectroscopic measurement with broadband FDML laser.

To reduce the influence of fluctuations in the optical output of the broadband FDML laser, the measurement signal was normalized using the reference signal. Furthermore, for spectroscopic measurements, the measurement results were converted from those based on time to wavelength based on the wavelength sweep characteristics of the broadband FDML laser obtained in Fig. 3. Figure 7 shows the results of spectral measurements compensating for the effects of light output fluctuations. Flat characteristics were obtained owing to the compensation of optical output fluctuation, and transmission spectra with five FBGs with different Bragg wavelengths were observed over a wide bandwidth ranging from 1500 to 1580 nm.

In Fig. 8, strain $\Delta\epsilon$ was applied to FBG₁, FBG₃, and FBG₅, and the change in transmission spectrum was measured to evaluate the performance of this experimental system. Strain was applied by stretching the optical fiber containing the FBG using a movable stage. Figure 8(a) shows the results of the spectroscopic measurement. The change in the transmission spectrum owing to the application of strain was evident in FBG₁, FBG₃, and FBG₅. Figure 8(b) shows the enlarged transmission spectrum of FBG₃. The peak spectral reflection wavelength values for $\Delta\epsilon = 0, 500$, and $1000 \mu\epsilon$ were 1540.43, 1541.00, and 1541.52 nm, respectively. Further,

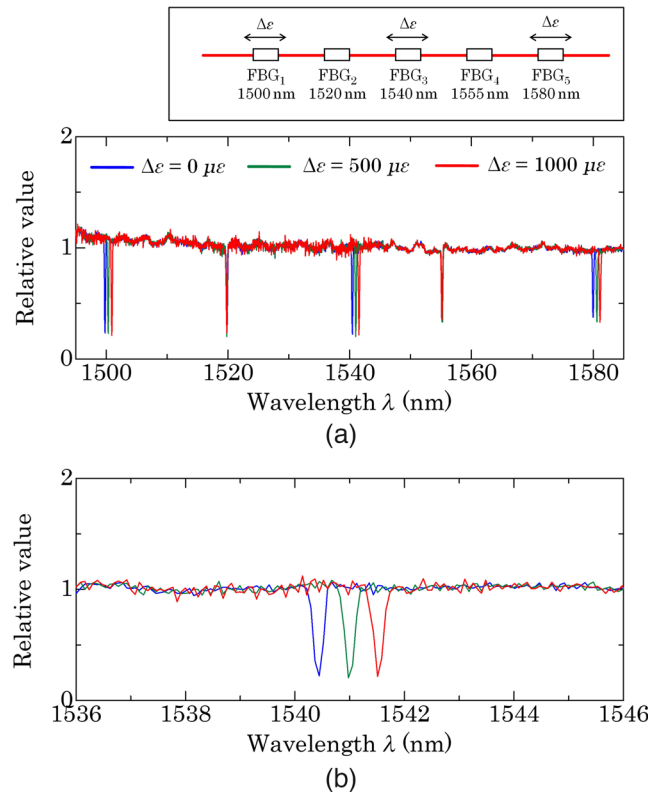


Fig. 8 Measurement of spectral changes when strains are applied to FBG₁, FBG₃, and FBG₅. (a) Results of spectroscopic measurements and (b) results of expanding (a) near FBG₃.

the analysis of the transmission spectra using Gaussian fitting (LabVIEW, National Instruments) revealed that the FBG₃ peak spectra for $\Delta\varepsilon = 0, 500, \text{ and } 1000 \mu\varepsilon$ had half-widths of $\sim 0.20, 0.20, \text{ and } 0.21 \text{ nm}$, respectively, and reflectance values of $83\%, 83\%, \text{ and } 79\%$, respectively, which were consistent with the FBG₃ specifications. Thus, the experiments confirmed that this experimental system can monitor slight changes in the transmission spectrum over a broad wavelength range.

4.2 Compensation for Wavelength Shift of Broadband FDML Laser

The effectiveness of this compensation method was verified by simulating the effect of wavelength shift on the broadband FDML laser. The experiment was tuned such that the wavelength shifts $\Delta\lambda_S$ were $\sim -1.28, 0, \text{ and } +1.28 \text{ nm}$, respectively, at the center wavelength of the broadband FDML laser of 1544 nm . This shift corresponded to $\sim 1\%$ of the wavelength sweep bandwidth of the laser. Figure 9(a) shows the results of the optical spectrum of the broadband FDML laser with OSA with an averaging count of 1. Figure 9(b) shows the results of the FBG_R reflection spectrum, which changed with the wavelength shift of the laser. The peak wavelengths of the respective reflection spectra of FBG_R at each wavelength shift were $1541.22, 1539.89, \text{ and } 1538.59 \text{ nm}$. Therefore, the wavelength shifts $\Delta\lambda_S$ can be calculated using Eq. (1) with results of Fig. 9(b) obtained as $-1.33, 0.00, \text{ and } +1.30 \text{ nm}$; these were almost identical to the adjusted wavelength of the broadband FDML laser.

Thereafter, spectroscopic measurements with wavelength shift compensation were performed. Figure 10(a) shows the spectroscopic measurement results before wavelength shift compensation. Originally, the spectra were supposed to be identical; however, they were shifted significantly owing to the wavelength shift of the broadband FDML laser. The peak wavelengths of the transmission spectra of FBG₃ were $1541.75, 1540.41, \text{ and } 1539.13 \text{ nm}$. Therefore, by setting the wavelength shift to $\Delta\lambda_S$, the peak wavelength was shifted by $-\Delta\lambda_S$. Figure 10(b)

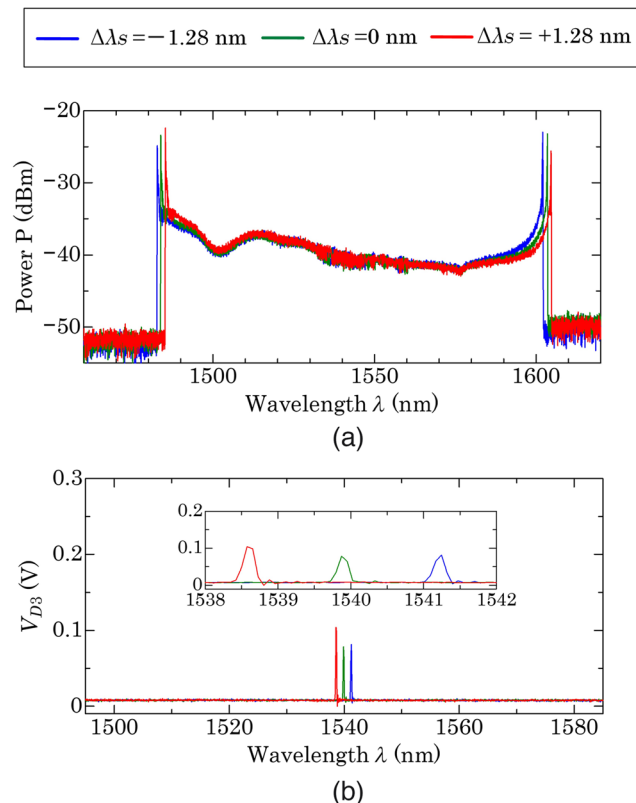


Fig. 9 Measurement results when the laser is wavelength-shifted. (a) Output spectrum of broadband FDML laser and (b) FBG_R reflection signal by compensation path.

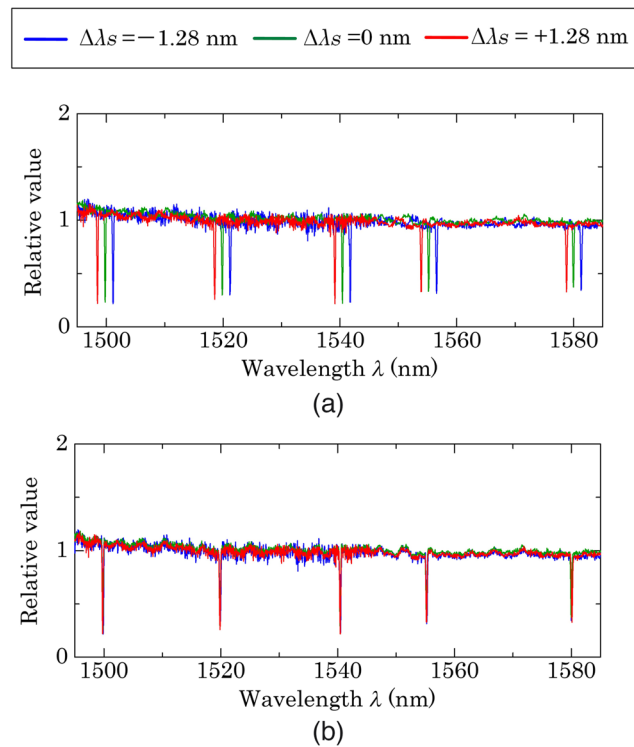


Fig. 10 Spectral measurements when the laser is wavelength-shifted. (a) Without compensation and (b) with compensation.

shows the results of wavelength shift compensation. The influence of the wavelength shift was reduced by the compensation of the FBG_R , and the transmission spectra of each FBG were measured as the same value. The peak wavelengths of the transmission spectra of FBG_3 were 1540.45, 1540.41, and 1540.43 nm, with improved values compared to Fig. 10(a).

The peak wavelengths of the transmission spectrum owing to static strain during wavelength shift were analyzed. Figure 11(i) shows the results before wavelength shift compensation. The experimental system could measure the linear response of the transmission spectra of FBG_1 , FBG_3 and FBG_5 owing to the application of strain. However, when affected by the wavelength shift amount $\Delta\lambda_S$, the measured wavelength was shifted by $-\Delta\lambda_S$ from the original FBG peak wavelength. Figure 11(ii) shows the results following wavelength shift compensation, and the same peak wavelength was obtained for the strain even if the wavelength shift was affected. The slope of the peak wavelength of each FBG with respect to strain was $\sim 1.2 \times 10^{-3} \text{ nm}/\mu\epsilon$. The standard deviation of the difference between the peak wavelengths obtained in Fig. 11(ii) without and with wavelength shift were <16, 14, and 61 pm for Figs. 11(a-ii), 11(b-ii), and 11(c-ii), respectively. The standard deviation is worse for Fig. 11(c-ii), which uses the end regions of the approximation equation in Fig. 3. This experimental system using the broadband FDML laser compensates for the wavelength shift effect and can simultaneously measure changes in multiple transmission spectra in the broadband range of 1500 to 1580 nm.

4.3 Evaluation of Fast Spectroscopic Measurements

To evaluate fast spectral measurements, a piezoelectric transducer with a vibration frequency of $f_v = 4.46 \text{ kHz}$ was installed in FBG_1 to change the transmission spectrum. The broadband FDML laser was set with a sweep period of $T_m = 19.7 \mu\text{s}$, and 100 irradiations were continuously performed for $\sim 2 \text{ ms}$. In addition, to verify the effect of wavelength shift compensation, the laser wavelength shifts $\Delta\lambda_S$ were adjusted to be ~ 0 , $+0.64$, and $+1.28 \text{ nm}$. Figures 12(a-i), 12(b-i), and 12(c-i) show the results of spectroscopic measurements with $\Delta\lambda_S = 0$, $+0.64$, and $+1.28 \text{ nm}$, respectively. Fast changes in the transmission spectrum owing to the application

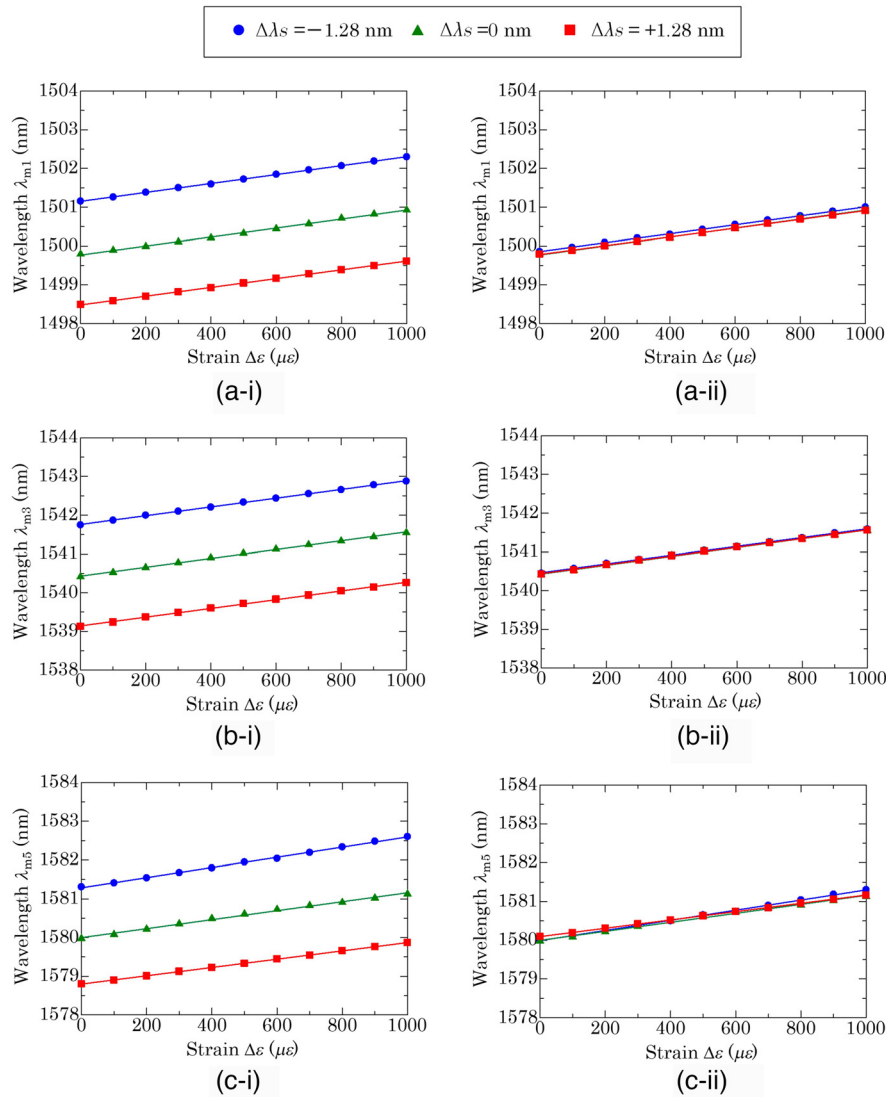


Fig. 11 Measurements of peak spectrum of FBGs by applying static strain. (i) Without compensation and (ii) with compensation. (a) FBG₁; (b) FBG₃; and (c) FBG₅.

of vibration to FBG₁ were observed. Figures 12(b-i) and 12(c-i), which are affected by wavelength shift, showed transmission spectra that were almost identical to Fig. 12(a-i) because of compensation.

Figure 12(ii) tracks the peak wavelength of the transmission spectrum of FBG₁. The experimental system clearly measured the sinusoidal variation of the peak wavelength with applied vibration frequency at a time resolution of 19.7 μ s. In Figs. 12(a-ii), 12(b-ii), and 12(c-ii), each vibration had a center wavelength of ~ 1499.25 nm and a peak-to-peak value of ~ 0.11 nm, indicating that almost identical peak wavelengths with compensation were obtained for the same vibrating body. The standard deviation of the peak wavelength of each FBG when no vibration was applied was <9 pm. Thus, the experimental system with the broadband FDML laser was demonstrated to be fast, broadband, and capable of performing spectroscopic measurements.

4.4 Considerations for Measurement Systems with Broadband FDML Laser with Two SOAs

The performance of the measurement system using the FDML laser with two SOAs was studied. First, two points were compared between a laser with one SOA¹³ and a laser with two SOAs:

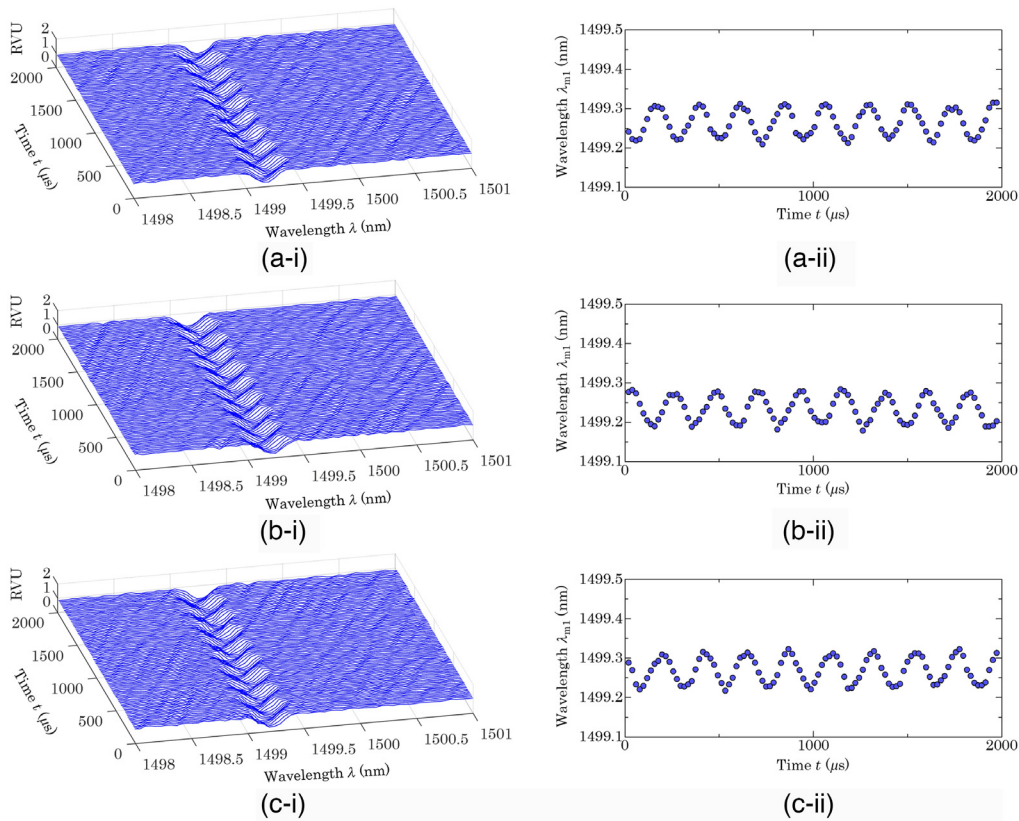


Fig. 12 Dynamic spectrum measurements with compensation by applying vibration with vibration frequency of 4.46 kHz. (i) time series spectrum of FBG₁. (ii) Results of peak tracking for FBG₁. (a) with $\Delta\lambda_S = 0$ nm; (b) with $\Delta\lambda_S = +0.64$ nm; and (c) with $\Delta\lambda_S = +1.28$ nm.

stability of optical output measurement and temporal stability of peak wavelength measurement. The stability of optical output measurement was evaluated by normalizing the light output in the spectral measurement shown in Fig. 7 and calculating the standard deviation. The wavelength interval for analysis was 1544 to 1549 nm. The laser with one SOA has a sweep bandwidth of 30 nm and a sweep rate of 50 kHz, and it was evaluated with the system developed in the previous study.¹³ The laser with two SOAs has a sweep bandwidth of 120 nm and a sweep rate of 50.7 kHz, and it was evaluated with the system developed in the present study. The ratio of the standard deviation was 0.8% for one SOA and 2.3% for two SOAs. While the laser with two SOAs was able to improve the sweep bandwidth, an increase in standard deviation for intensity was observed. The temporal stability of the peak wavelength measurement was evaluated by calculating the standard deviation from the time series results of the peak wavelength of each FBG. No vibration was applied to each FBG. When wavelength measurements were performed with one SOA and two SOAs, the standard deviations of the peak wavelengths were ~ 7 and 9 pm, respectively.

Next, we discuss the sweep rate of the FDML laser, which determines the measurement rate of the measurement system. FDML operation is known as a method of driving wavelength-swept lasers at fast sweep rates exceeding tens of kHz.¹² FDML operation requires that the time for light to circulate in the resonator be synchronized with the driving period of the wavelength filter. Here, since the developed FDML laser has two SOAs in parallel, matching the circumnavigation time of light in the two optical paths is necessary. Therefore, in this experiment, each optical path length is adjusted in cm units, and the laser is designed so that the circumnavigation time of each optical path is equal. The maximum sweep rate of the FDML laser is limited by the wavelength filter. Most wavelength filters used for FDML lasers are FFP-TF. These filters mechanically control the wavelength by means of piezoelectric actuator. This limits the operating sweep rate to a several tens of kHz. To overcome this limitation, lasers with

buffered optics have recently been proposed.²³ This method multiplexes the laser sweep and can further increase the sweep rate by a factor of several. Therefore, the developed FDML laser is expected to increase the current measurement rate by several times by introducing the latest buffered optics.

The FDML laser has proven to be useful for gas spectroscopy and other applications, while being relatively inexpensive compared to light sources typically used for high-speed spectroscopy. By introducing FDML operation and two SOAs in parallel, the proposed broadband FDML laser has a sweep bandwidth of 120 nm at a center wavelength of 1544 nm and a fast sweep rate of 50.7 kHz. The experiments were thorough and systematic, and provide the basic design for the development of the measurement system. Using FDML and two SOAs is a very innovative way to extend the sweep bandwidth to 120 nm in the 1.55- μm wavelength band. In addition, a simple wavelength-shift compensation method for long-time operation of lasers will contribute to further performance enhancement of spectral measurement systems. These results are impressive and will be of interest to the broad community working on fast wavelength-swept lasers and their applications.

5 Conclusion

This study developed an experimental system using the broadband wavelength-swept laser to realize broadband and fast spectroscopic measurements at ~ 1550 nm. The broadband wavelength-swept laser overcame the limitations of sweep speed and sweep bandwidth by introducing FDML operation and parallelization of two SOAs. The proposed broadband FDML laser has a sweep bandwidth of 120 nm at a center wavelength of 1544 nm as well as a high-speed sweep rate of 50.7 kHz. The experimental system used reference and compensation optics to compensate for variations in the optical output and wavelength shift of the laser. Further, spectroscopic measurements showed a change in the transmission spectrum over a broadband range of 1500 to 1580 nm. Fast spectroscopic measurements demonstrate that steep transmission spectral changes due to FBG can be observed with a temporal resolution of 19.7 μs with a standard deviation of 9 pm. In future, the authors plan to replace the measurement optical path of this experimental system with a gas cell and apply it to the acquisition of gas absorption spectra. In actual spectroscopic measurements using a gas cell, the line width of the absorption spectrum of a gas varies with pressure. In future, we plan to verify whether the measurement system can observe the change in the line width of the gas.

Acknowledgments

This work was partly supported by the JSPS KAKENHI (Grant No. 20K14754) and by the Nihon University College of Science and Technology for Research.

References

1. H. Büning-Pfaue et al., "Analysis of water in food by near infrared spectroscopy," *Food Chem.* **82**(1), 107–115 (2003).
2. J. Luybaert, D. L. Massart, and Y. Vander Heyden, "Near-infrared spectroscopy applications in pharmaceutical analysis," *Talanta* **72**(3), 865–883 (2007).
3. A. Sakudo, "Near-infrared spectroscopy for medical applications: current status and future perspectives," *Clin. Chim. Acta* **455**(1), 181–188 (2016).
4. C. Pasquini, "Near infrared spectroscopy: A mature analytical technique with new perspectives – a review," *Anal. Chim. Acta* **1026**(5), 8–36 (2018).
5. W. Ren et al., "CO concentration and temperature sensor for combustion gases using quantum-cascade laser absorption near 4.7 μm ," *Appl. Phys. B* **107**, 849–860 (2012).
6. C. S. Goldenstein et al., "Infrared laser-absorption sensing for combustion gases," *Prog. Energy Combust. Sci.* **60**, 132–176 (2017).
7. O. Witzel et al., "VCSEL-based, high-speed, in situ TDLAS for in-cylinder water vapor measurements in IC engines," *Opt. Express* **21**(17), 19951–19965 (2013).

8. N. G. Blume and S. Wagner, "Broadband supercontinuum laser absorption spectrometer for multiparameter gas phase combustion diagnostics," *Opt. Lett.* **40**(13), 3141–3144 (2015).
9. G. B. Rieker et al., "Frequency-comb-based remote sensing of greenhouse gases over kilometer air paths," *Optica* **1**(5), 290–298 (2014).
10. R. J. Tancin and C. S. Goldenstein, "Ultrafast-laser-absorption spectroscopy in the mid-infrared for single-shot, calibration-free temperature and species measurements in low- and high-pressure combustion gases," *Opt. Express* **29**(19), 30140–30154 (2021).
11. L. A. Kranedonk et al., "High speed engine gas thermometry by Fourier-domain mode-locked laser absorption spectroscopy," *Opt. Express* **15**(23), 15115–15128 (2007).
12. R. Huber, M. Wojtkowski, and J. G. Fujimoto, "Fourier domain mode locking (FDML): a new laser operating regime and applications for optical coherence tomography," *Opt. Express* **14**(8), 3225–3237 (2006).
13. T. Yamaguchi, W. Endo, and Y. Shinoda, "Real-time spectroscopy system for continuous measurement with Fourier-domain mode-locked laser at 1550 nm," *IEEE Sens. Lett.* **5**(8), 1–4 (2021).
14. M. Y. Jeon et al., "High-speed and wide bandwidth Fourier domain mode-locked wavelength swept laser with multiple SOAs," *Opt. Express* **16**(4), 2547–2554 (2008).
15. S. H. Kassani et al., "Extended bandwidth wavelength swept laser source for high resolution optical frequency domain imaging," *Opt. Express* **25**(7), 8255–8266 (2017).
16. J. G. Mance et al., "Time-stretch spectroscopy for fast infrared absorption spectra of acetylene and hydroxyl radicals during combustion," *Opt. Express* **28**(20), 29004–29015 (2020).
17. J. M. López-Higuera, *Handbook of Optical Fibre Sensing Technology*, Wiley, Hoboken, NJ, USA (2002).
18. R. Isago and K. Nakamura, "A high reading rate fiber Bragg grating sensor system using a high-speed swept light source based on fiber vibrations," *Meas. Sci. Technol.* **20**(3), 034021 (2009).
19. K. Yuksel et al., "Complete analysis of multireflection and spectral-shadowing crosstalks in a quasi-distributed fiber sensor interrogated by OFDR," *IEEE Sens. J.* **12**(5), 988–995 (2012).
20. T. Yamaguchi and Y. Shinoda, "Real-time fiber Bragg grating measurement system using temperature-controlled Fourier domain mode locking laser," *Opt. Eng.* **56**(6), 066112 (2017).
21. T. Yamaguchi, W. Endo, and Y. Shinoda, "High-speed interrogation system for fiber Bragg gratings with buffered Fourier domain mode-locked laser," *IEEE Sens. J.* **21**(15), 16659–16669 (2021).
22. T. Yamaguchi, A. Nakamoto, and Y. Shinoda, "Real-time measurement system for overlapping reflection signals of fiber Bragg gratings using high-speed wavelength-swept laser," *Opt. Eng.* **61**(7), 076114 (2022).
23. R. Huber et al., "Buffered Fourier domain mode locking: unidirectional swept laser sources for optical coherence tomography imaging at 370,000 lines/s," *Opt. Lett.* **31**(20), 2975–2977 (2006).

Tatsuya Yamaguchi received his BS, MS, and PhD degrees in engineering from Nihon University, Tokyo, Japan, in 2013, 2015, and 2018, respectively. He then joined the Department of Electrical Engineering at Nihon University. His current research interests include optical measurements, digital signal processing, and optical fiber sensing. He is a member of the Institute of Electrical Engineers of Japan (IEEJ), Society of Instrument and Control Engineers (SICE), Institute of Electrical and Electronics Engineers (IEEE), and Society of Photographic Instrumentation Engineers (SPIE).

Akira Nakamoto received his BS and MS degrees in engineering from Nihon University, Tokyo, Japan, in 2020 and 2022, respectively. He has been employed by Nihon Kohden Corporation. His current research interest includes optical fiber sensing.

Yukitaka Shinoda received his BSc, MSc, and PhD degrees in electrical engineering from Nihon University in 1987, 1989, and 2004, respectively. He was a visiting researcher at the Virginia Polytechnic Institute and State University (Virginia Tech) from 2009 to 2010. Since 2012, he has been a professor at the College of Science and Technology, Nihon University. He has focused on laser sensing, digital signal processing, motion analysis, and optical scanning holography. He is a member of the Institute of Electrical Engineers of Japan (IEEJ), the Society of Instrument and Control Engineers (SICE), the Japan Society of Applied Physics (JSAP), and Institute of Electrical and Electronics Engineers (IEEE).